# ANFIS CONTROLLED PLUG-IN HYBRID ELECTRIC VEHICLE

[1]G.Varshith [2]B.Pavan Kumar Reddy [3]B.Kavya Sree Reddy
[1]Graduate in Electrical & Electronics Engineering, Sree Vidyanikethan Engineering College
[2]Post Graduate in Power Electronics & Electrical Drives
[3]Graduate in Electrical & Electronics Engineering, National Institute of Technology, Puducherry

## Abstract

Hybrid Electric vehicle (HEV) technology gives a viable answer for accomplishing higher fuel economy and better exhibitions with diminished green house gas emissions. For Electric vehicle applications, Switched reluctance motor (SRM) is the best reasonable one of all the accessible motors. To increase the driving miles of the electric vehicles, a photovoltaic (PV) panel is mounted alongside on-board battery bank. A tri-port converter with Adaptive Neuro Fuzzy Inference controller (ANFIS) is proposed in this paper to control the energy flow between the PV panel, battery and SRM drive. Six operational modes are introduced, four of which are produced for driving modes and rest two for stop on-board charging. In driving modes, the Perturb and watch system is utilized so as to get greatest power from the PV panel. In standstill charging modes, a matrix associated charging topology is created with no outside equipment. A multi area charging control procedure is utilized adversary viable use of vitality if there should be an occurrence of battery charging from PV panel straightforwardly. The proposed tri port technology with Adaptive Neuro Fuzzy Inference controller (ANFIS) is developed in MATLAB/SIMULINKenvironment and the results are proven to be successful in producing reduced harmonic distortion and have the capability to make better market for electric vehicle in the nearby future.

**Index Terms** - Electric Vehicles, Photovoltaic (PV), Switched Reluctance Motors (SRMs), Tri-Port Converter, Perturb and Observe Technique, Adaptive Neuro fuzzy Inference Controller.

## I. INTRODUCTION

Electric vehicles have taken a significant leap forward, by advances in motor drives, power converters, batteries andenergy management systems [1]-[4]. Be that as it may, due to thelimitation of current battery technologies, the driving miles is moderately short that limits the wide utilization of EVs [5]-[7]. In terms of motor drives, high-performance permanent-magnet (PM) machines are generally utilized while rare-earth materials are required in large quantities, restricting the wide utilization of EVs. Keeping in mind the end goal to defeat these issues, a photovoltaic panel and a switched reluctance motor (SRM) are introduced with give power supply and motor drive, respectively. Firstly, by including the PV panel on top of the EV, a sustainable energy source isachieved. Nowadays, a typical passenger car has a surface enough to install a 250-W PV panel. Second, a SRM needs no rare-earth PMs and is additionally robust so it gets increasing attention in EV applications. While PV panels have low power density for traction drives, they can be used to charge batteries the greater part of time. For the most part, the PV-fed EV has a comparable structure to the hybrid electrical vehicle, whose internal combustion engine(ICE) is supplanted by the PV panel. The PV-fed EV system is outlined in Fig. 1. Its key components include an off-board charging station, a PV, batteries and power converters. In order to decrease the energy conversion processes, one approach is to upgrade the motor to include some on-board charging functions. For example, paper designs a 20-kW split-phase PM motor for EV charging, yet it endures from high harmonic contents in the back electromotive drive (EMF). Another solution depends on a traditional SRM. Paper achieves on-board charging and power factor correction in

a 2.3-kW SRM by utilizing machine windings as the input filter inductor. The concept of modular structure of driving topology is proposed in paper. Based on intelligent power modules (IPM), a four-phase half bridge converter is utilized to achieve driving and grid-charging. In spite of the fact that modularization supports mass production, the utilization of half/full bridge topology reduces the system reliability (e.g. shoot-through issues). Paper builds up a basic topology for plug-in hybrid electrical vehicle (HEV) that supports flexible energy flow. In any case, for grid charging, the grid should be associated with the generator rectifier that builds the energy conversion process and decreases the charging efficiency. In any case, a powerful topology and control strategy for PV-fed EVs is not yet developed. Since the PV has different characteristics to ICEs, the maximum power point tracking (MPPT) and solar energy utilization are the unique factors for the PV-fed EVs.

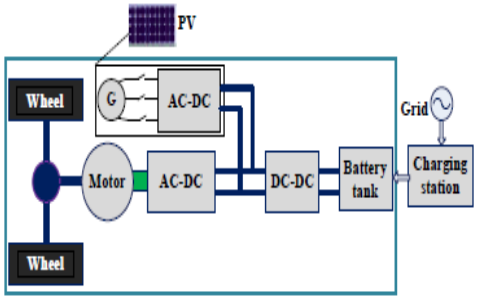


**Fig. 1 PV-fed hybrid electrical vehicle.**

In order to achieve low cost and flexible energy flow modes, a low cost tri-port converter is proposed in this paper to arrange the PV panel, SRM and battery. Six operational modes are developed to support flexible control of energy flow.

## II. TOPOLOGY AND OPERATIONAL MODES

### A. Proposed topology and working modes

The proposed Tri-port topology has three energy terminals, PV, battery and SRM. They are linked by a power converter which comprises of four switching devices (S0~S3), four diodes (D0~D3) and two relays, as appeared in Fig. 2 [26]. By controlling relays J1 and J2, the six operation modes are upheld, as appeared in Fig. 3; the corresponding relay activities are delineated in Table I. In mode 1, PV is the energy source to drive the SRM and to charge the battery. In mode 2, the PV and battery are both the energy sources to drive the SRM. In mode 3, the PV is the source and the battery is idle. In mode 4, the battery is the driving source and the PV is idle. In mode 5, the battery is charged by a single-phase grid while both the PV and SRM are idle. In mode 6, the battery is charged by the PV and the SRM is idle.

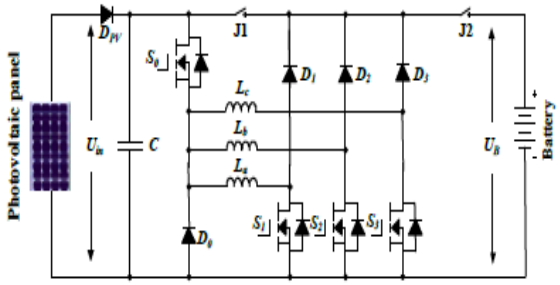


**Fig. 2. The proposed Tri-port topology for PV-powered SRM drive.**

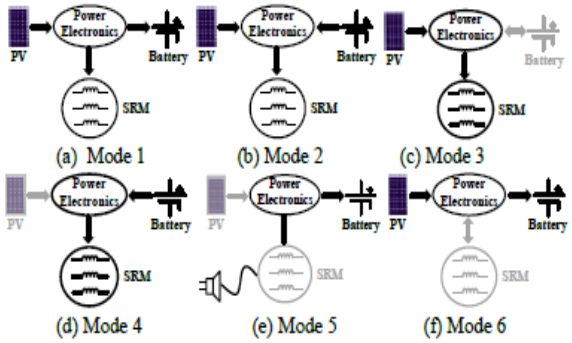


**Fig. 3. Six operation modes of the proposed Tri-port topology.**

TABLE I J1 and J2 Actions under Different Modes

| Mode | J1 and J2 |
|---|---|
| 1 | J1 turn-off; J2 turn-on |
| 2 | J1 and J2 turn-on |
| 3 | J1 turn-on; J2 turn-off |
| 4 | J1 and J2 turn-on |
| 5 | J1 and J2 turn-on |
| 6 | J1 turn-off; J2 turn-on |

**B. Driving modes**

Working modes 1~4 are the driving modes to give traction drive to the vehicle.

**(1) Mode 1**

At light loads of operation, the energy produced from the PV is more than the SRM required; the system works in mode 1. The corresponding operation circuit is appeared in Fig.4 (an), in which relay J1 turns off and relay J2 turns on. The PV panel energy feed the energy to SRM and charge the battery; so in this mode, the battery is charged in EV operation condition.

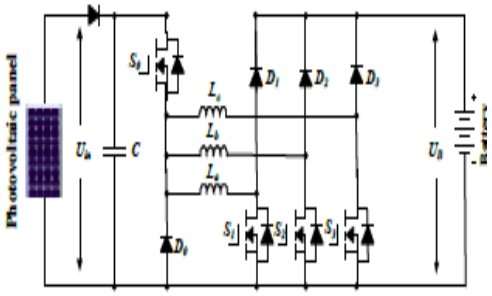


**(a) Operation circuit under mode 1**

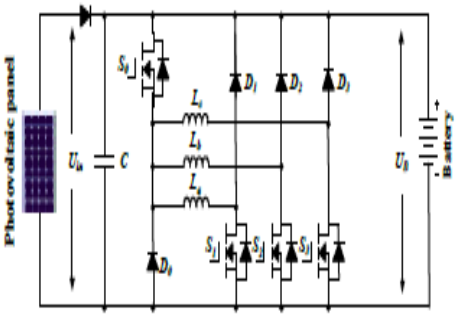


**(b) Operation circuit under mode 2**

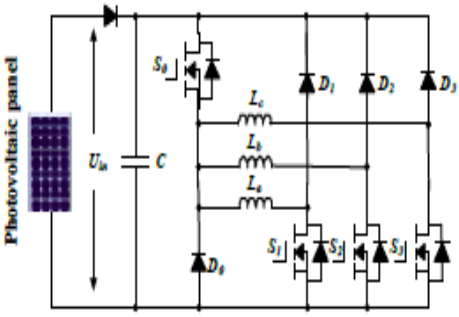


**(c)Operation circuit under mode 3**

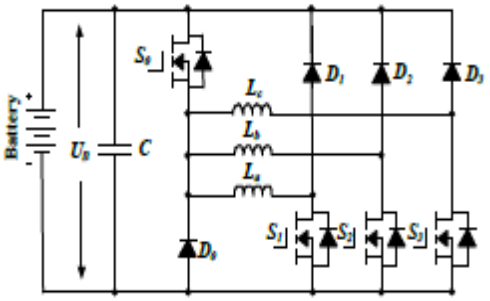


**(d) Operation circuit under mode 4**

Fig. 4 the equivalent circuits under driving modes.

**(2) Mode 2**

At the point when the SRM operates in heavy load, for example, uphill drivingor acceleration, both the PV panel and battery supply power tothe SRM. The relating operation circuit is appeared in Fig. 4(b), in which relay J1 and J2 are turned on.

**(3) Mode 3**

At the point when the battery is out of power, the PV panel is the onlyenergy source to drive the vehicle. The corresponding circuit is appeared in Fig. 4(c). J1 turns on and J2 turns off.

**(4) Mode 4**

At the point when the PV can't generate electricity due to low solarirradiation, the battery supplies power to the SRM. The corresponding topology is delineated in Fig. 4(d). In this mode, relay J1 and J2 are both conducting.

**C. Battery charging modes**

Operating modes 5 and 6 are the battery charging modes.

**(5) Mode 5**

At the point when PV can't generate electricity, an external powersource is expected to charge the battery, for example, AC grid. The relating circuit is appeared in Fig. 5(a). J1 and J2 turns on. Point Anis central tapped of phase windings that can be effectively accomplished without changing the motor structure. One of the three phase windings is split and its midpoint is pulled out, as appeared in Fig. 5(a). Phase windings La1

and La2 are employed as inputfilter inductors. These inductors are a part of the drive circuit to form an AC-DC rectifier for grid charging.

**(6) Mode 6**

At the point when the EV is stopped under the sun, the PV can charge the battery. J1 turns off; J2 turns on. The relating charging circuit is appeared in Fig. 5(b).

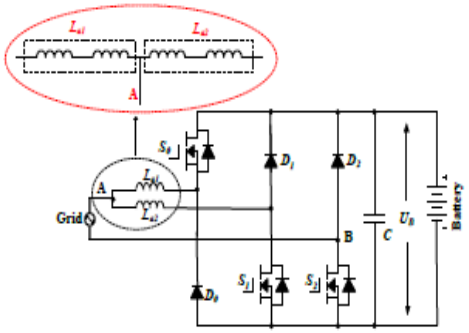


(a) **Grid charging mode**

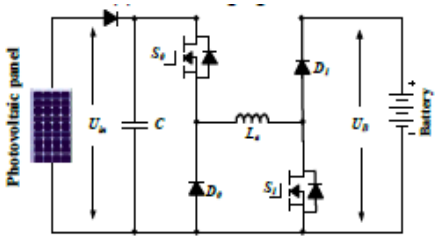


**(b) PV source charging mode**

**Fig. 5 Equivalent circuits of charging condition modes.**

## III. CONTROL STRATEGY UNDER DIFFERENT MODES

In order to make the best utilization of sun oriented energy for driving the EV, a control strategy under various modes is planned.

### A. Single source driving mode

As indicated by the distinction in the power sources, there are PV-driving; battery-driving and PV and battery parallel fed source. In a heavy load condition, the PV power can't support the EV, mode 2 can be adopted to support enough energy and make full utilization of solar energy. Fig. 6(a) demonstrates the equivalent power source; the corresponding PV panel working points is represented in Fig. 6(b). Since the PV is paralleled with the battery, the PV panel voltage is clamped to the battery voltage UB. In mode 2, there are three working states: winding excitation, energy recycling and freewheeling states, as appeared in Fig. 7. Modes 3 and 4 have comparable working states to mode 2. The difference is that the PV is the only source in mode 3 while the battery is the only source in mode 4.

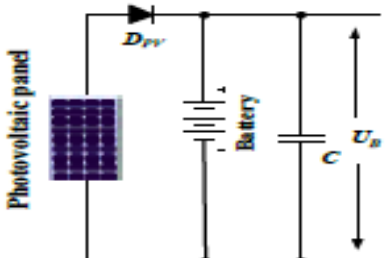


**(a) Compound power source**

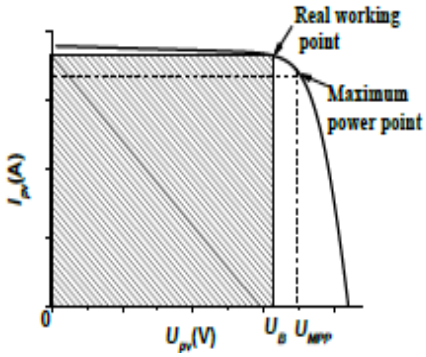


**(b) Working point of the PV**

**Fig. 6 Power supply at mode 2.**

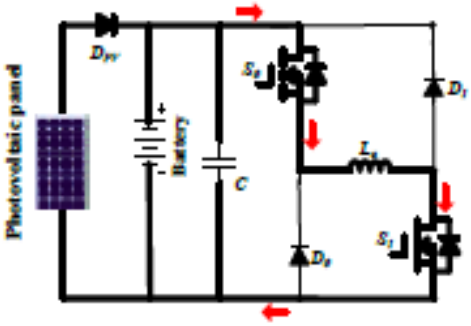


**(a) Winding excitation state**

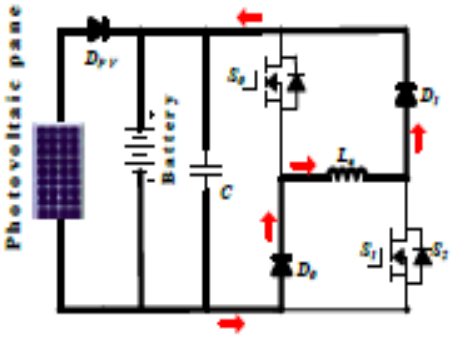


**(b) Energy recycling state**

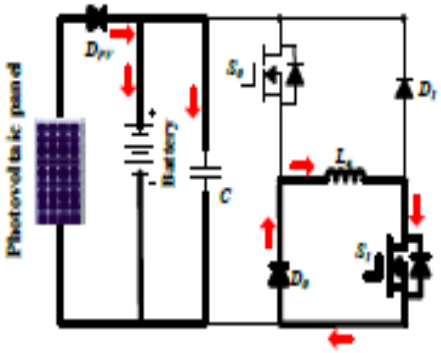


**(c) Freewheeling state**

Fig. 7 Working states at mode 2.

Neglecting the voltage drop over the power switches and diodes, the phase voltage is given by

$$U_{in} = R_k i_k + \frac{d\psi(i_k,\theta_r)}{dt} = R_k i_k + L_k \frac{di_k}{dt} + i_k \omega_r \frac{dL_k}{d\theta_r}, \quad k = a,b,c \tag{1}$$

where Uin is the DC-link voltage, k is phase a, b, or c, Rk is the phase resistance, ik is the phase current, Lk is the phase inductance, θr is the rotor position, ψ(ik, θr) is the phase flux linkage depending upon the phase current and rotor position, and ωr is the angular speed.

The third term in Eq. 1 is the back electromotive force (EMF) voltage by

$$e_k = i_k \omega_r \frac{dL_k}{d\theta_r} \tag{2}$$

Consequently, the phase voltage is found by

$$U_k = R_k i_k + L_k \frac{di_k}{dt} + e_k \tag{3}$$

In the excitation area, turning on S0 and S1 will induce a current in phase a winding, as show in Fig. 7(a). Phase a winding is subjected to the positive DC bus voltage.

$$+U_{in} = R_k i_k + L_k \frac{di_k}{dt} + e_k \tag{4}$$

At the point when S0 is off and S1 is on, the phase current is in a freewheeling state in a zero voltage loop, as appeared in Fig. 7(c), the phase voltage is zero.

$$0 = R_k i_k + L_k \frac{di_k}{dt} + e_k \tag{5}$$

In the demagnetization region, S0 and S1 are both turned off; what's more, the phase current will flow back to the power supply, as appear in Fig. 7(b). In this state, the phase winding is subjected to the negative DC bus voltage, and the phase voltage is

$$-U_{in} = R_k i_k + L_k \frac{di_k}{dt} + e_k \tag{6}$$

In single source driving mode, the voltage-PWM control is utilized as the fundamental plan, as showed in Fig. 8. As per the given speed ω*, the voltage-PWM control is activated at speed control.

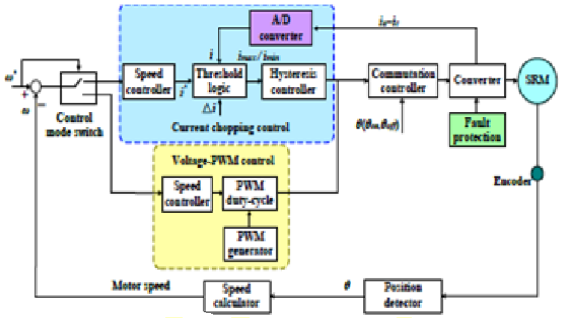


**Fig. 8. SRM control strategy under single source driving mode.**

### B. Driving-charging hybrid control strategy

In the driving-charging hybrid control, the PV is the driving source and the battery is charged by the freewheeling current, as represented in drive mode 1. There are two control targets: maximum power point tracking (MPPT) of the PV panel and speed control of the SRM. The dual-source condition is switched from a PV-driving mode. Firstly, the motor speed is controlled at a given speed in mode 3. At that point, J2 is turned on and J1 is off to switch to mode 1. By controlling the turn-off point, the maximum power of PV panel can be tracked. There are three steady working states for the double source (mode 1), as appeared in Fig. 9. In Fig. 9(a), S0 and S1 conduct, the PV panel charges the SRM winding to drive the motor; In Fig. 9(b), S0 and S1 turn off; and the battery is charged with freewheeling current of the phase winding. Fig. 9(c) appears a freewheeling state.

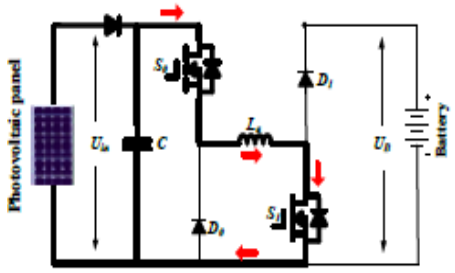


**(a) Winding exciting state**

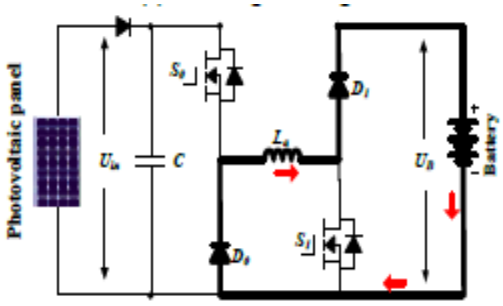


**(b) Battery charging state**

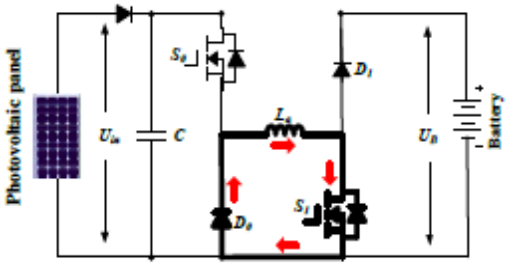


**(c).Freewheeling state**

**Fig. 9 Mode 1 working states.**

Fig.10 is the control strategy under driving-charging mode. In Fig.10, $\theta_{on}$ is the turn on angle of SRM; $\theta_{off}$ is the turn-off angle of SRM. By changing turn-on angle, the speed of SRM can be controlled; the maximum power point tracking of PV panel can be achieved by adjusting turn-off angle, which can control the charging current to the battery.

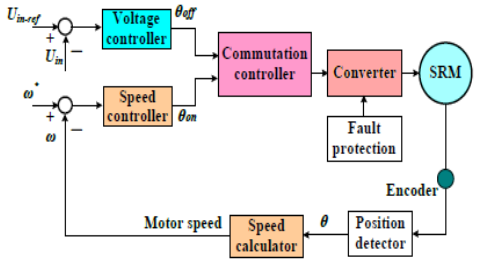


**Fig. 10. Control strategy under driving-charging mode (mode 1)**

### C. Grid-charging control system

The proposed topology also supports the single-phase grid charging. There are four fundamental charging states and S0 is dependably turned off. At the point when the grid instantaneous voltage is more than zero, the two working states are exhibited in Fig. 11(a) and (b). In Fig. 11(a), S1 and S2 conduct, the grid voltage charges the phase winding La2, the relating condition can be communicated as Eq.7; In Fig. 11(b), S1 turns off and S2 conducts, the grid is associated in series with phase winding to charges the battery, the relating condition can be communicated as Eq. 8.

$$U_{grid} = L_{a2} \cdot \frac{di_{grid}}{dt} \quad (7)$$

$$U_B - U_{grid} = L_{a2} \cdot \frac{di_{grid}}{dt} \quad (8)$$

At the point when the grid instantaneous voltage is below zero, the two working states are introduced in Fig. 11(c) and (d). In Fig. 11(c), S1 and S2 conduct, the grid voltage charges the phase winding La1 and La2, the comparing condition can be communicated as Eq. (9); In Fig. 11(d), S1 continues conducing and S2 turns off, the grid is associated in series with phase winding La1 and La2 to charges the battery, the relating condition can be communicated as Eq. 10.

$$U_{grid} = \frac{L_{a1} + L_{a2}}{L_{a1} \cdot L_{a2}} \cdot \frac{di_{grid}}{dt} \quad (9)$$

$$-U_B - U_{grid} = \frac{L_{a1} + L_{a2}}{L_{a1} \cdot L_{a2}} \cdot \frac{di_{grid}}{dt} \quad (10)$$

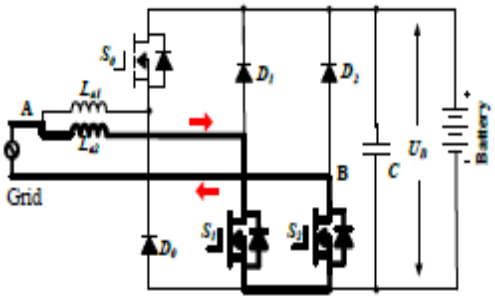


**(a) Grid charging state 1 (*Ugrid*>0)**

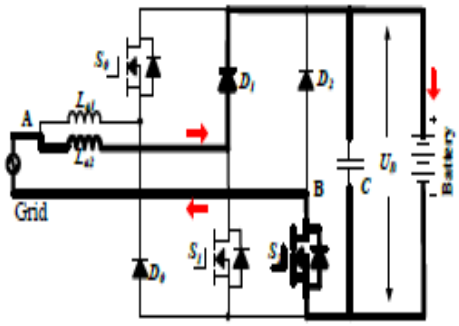


**(b) Grid charging state 2 (*Ugrid*>0)**

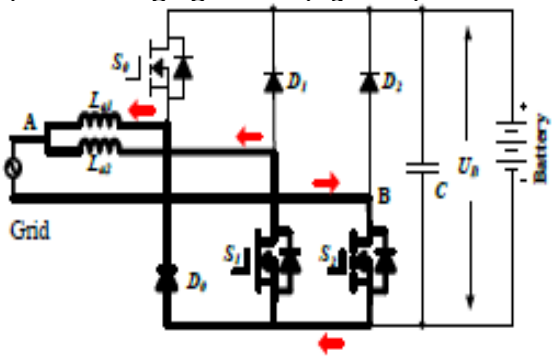


**(c) Grid charging state 3 (*Ugrid*<0)**

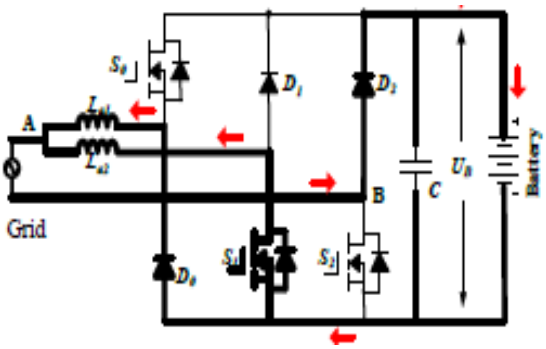


**(d) Grid charging state 4 (*Ugrid*<0)**

**Fig.11 Mode 5 charging states .**

In Fig. 12, Ugrid is the grid voltage; by the phase lock loop (PLL), the phase data can be got; Iref_grid is the given amplitude of the grid current. Combining sinθ and Iref_grid, the instantaneous grid current reference iref_grid can be figured. In this mode, when Ugrid> 0, the inductance is La2; when Ugrid< 0, the inductance is paralleled La1 and La2; so in order to adopt the change in the inductance, hysteresis control is employed to acknowledge grid current regulation. Besides, hysteresis control has great loop performance, global stability and small phase lag that makes grid connected control stable

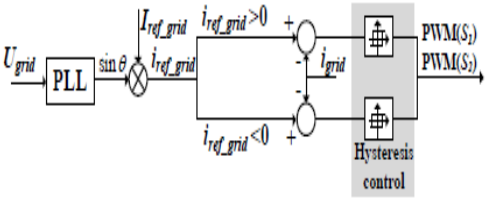


**Fig. 12 Grid-connected charging control (Mode 5).**

**D. PV-fed charging control system**

In this mode, the PV panel charges the battery specifically by the driving topology. The phase windings are employed as inductor; what's more, the driving topology can be worked as interleaved Buckboost charging topology. For one phase, there are two states, as appeared in Fig. 13(a) and (b). Whenever S0 and S1 turn on, the PV panel charges phase inductance; when S0 and S1 turns off, the phase inductance discharges energy to battery. According to the state-of-charging (SoC), there are three stages to make full utilize of solar energy and keep up battery

healthy condition, as represented in Fig.13 (c). During stage 1, the relating battery SoC is in 0~SoC1, the battery is in greatly need energy condition, the MPPT control strategy is utilized to make full utilization of solar energy. During stage 2, the corresponding battery SoC is in SoC1~ SoC2, the constant voltage control is adapted to charging the battery. During stage 3, the corresponding battery SoC is in SoC2~1, the micro current charging is adapted. In order to simplify the control strategy, constant voltage is employed in PV panel MPPT control.

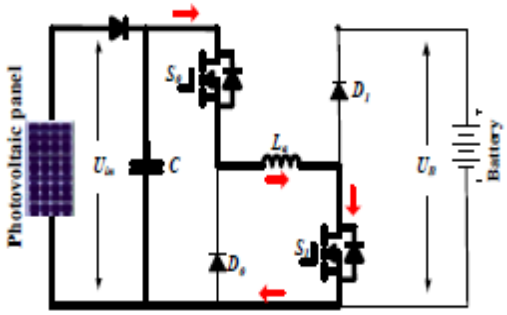


**(a) Phase inductance charging**

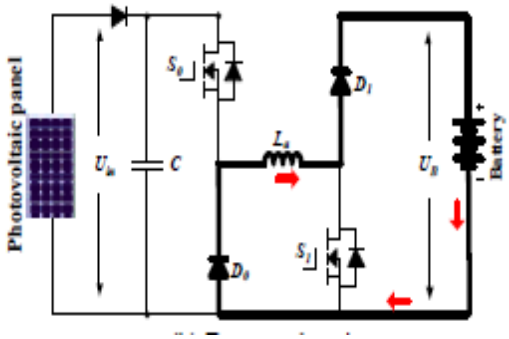


**(b) Battery charging**

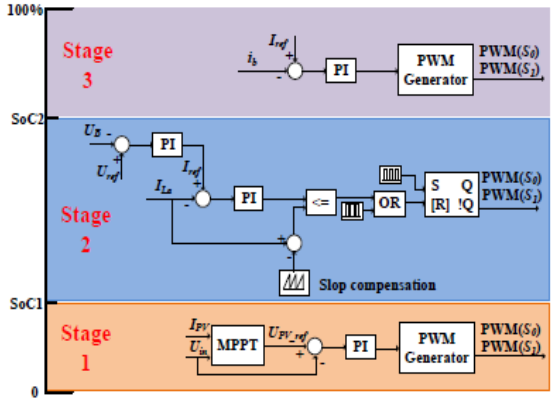


**(c) Charging control strategy.**

Fig. 13 Mode 6 charging states and control strategy.

## EXTENSION

### Adaptive Neuro Fuzzy Inference System

This is a neuro fuzzy technique where the fusion is made between the neural network and the fuzzy inference system, usually have the advantage of allowing an easy translation of the final system into a set of if-then rules, and the fuzzy system can be viewed as a neural network structure with knowledge distributed throughout connection strengths. Research and applications on neuro-fuzzy inference strategy made clear that neural and fuzzy hybrid systems are beneficial in fields such as the applicability of existing algorithms for artificial neural networks (ANNs), and direct adaptation of knowledge articulated as a set of fuzzy linguistic rules. An adaptive network, as its name implies, is a network structure consisting of nodes and directional links, overall input-output behavior is determined by the values of a collection of modifiable parameters through which the nodes are connected. The adaptive system uses a hybrid learning algorithm to identify parameters of Sugeno-type fuzzy inference systems. It applies a combination of the least-squares method and the back-propagation gradient descent method for training FIS membership function parameters to emulate a given training data set.The network learns in two main phases. In the forward phase of the learning algorithm, consequent parameters identify the least squares estimate. In the backward phase, the error signals, which are the derivatives of the squared error with respect to each node output, propagate backward from the output layer to the input layer. In this backward pass, the premise parameters are updated by the gradient descent algorithm. Learning or training phase of the neural network is a process to determine parameter values to sufficiently fit the training data. ANFIS training can use alternative algorithms to reduce the error of the training. A combination of the gradient descent algorithm and a least squares algorithm is used for an effective search for the optimal parameters. The main benefit of such a hybrid approach is that it converges much faster, since it reduces the search space dimensions of the backpropagation method used in neural networks. ANFIS are the fuzzy Sugeno model put in framework of the adaptive system which serves in model building

and validation of developed model to facilitate training and adaptation.

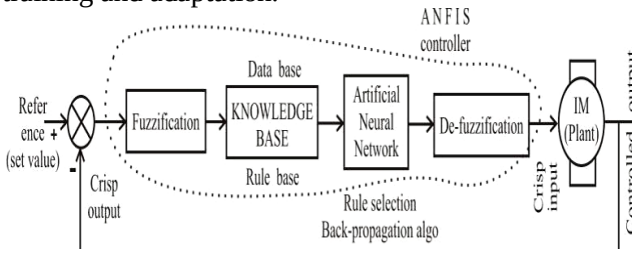


**Fig. 14 Block diagram of the ANFIS control scheme**

## IV. SIMULATION

A 12/8 SRM is initially modeled in Matlab/Simulink utilizing parameters in Table II. Fig. 15(a) presents the simulation results at mode 1. The load torque is set as 35 Nm, the PV panelvoltage is controlled at the MPP. The freewheeling current is used to charge the battery. Fig. 15(b) demonstrates the simulationresults of the single-source driving (modes 2-4).

Table II : Simulation Parameters

| Parameter | Value |
|---|---|
| SRM | 12/8 |
| PV panel<br>Maximum power point voltage reference voltage | 310 V |
| Battery voltage | 350 V |
| Constant voltage control reference voltage | 355 V |
| Constant current control reference current | 1 A |
| Mode 1, charging current | 60 A |
| Mode 4, driving speed | 1250 rpm |
| Mode 6, constant voltage charging reference | 355 V |
| Mode 6, constant current charging reference | 1 A |

Fig. 16 demonstrates the simulation results of charging where Fig. 16(a) is for grid-charging. The positive half current quality is superior to anything the negative half that is caused by the change in thegrid-connected inductance.Fig.16(b) and (c) are for PV-charging. Fig. 16(b) presents the step change from stage 1 to 2.

In stage 1, the battery is low in SoC. In order to achieve MPPT of the PV, the constant voltage control is utilized and the PV output voltage is controlled at MPP (310 V), as appeared in Fig. 16(b). In stage 2, a constant voltage is embraced; the reference voltage is set to 355 V. As appeared in Fig. 16(b), the charging converter output voltage is controlled at reference voltage in the step change from stage 1 to stage 2. In stage 3, 1 A trickle charging is moreover accomplished, as appeared in Fig. 16(c).

### Mode 1

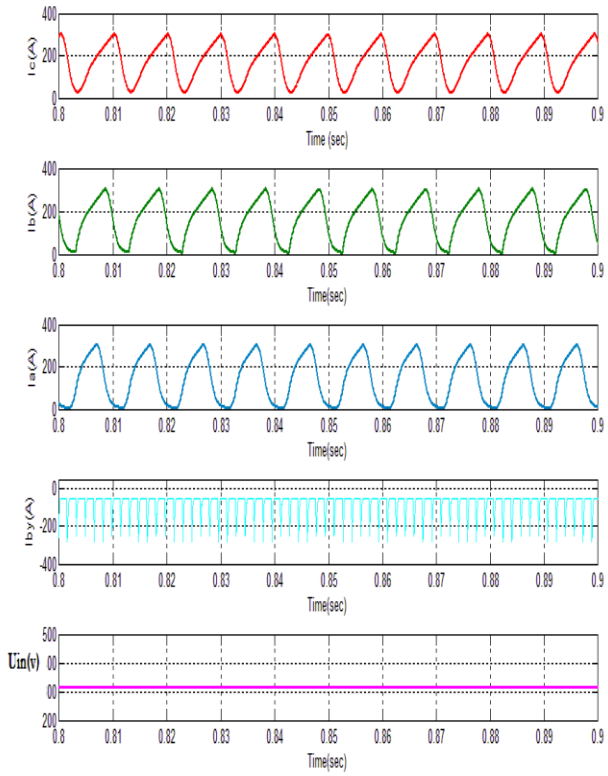


**(a) Simulation results of driving-charging mode (mode 1)**

**Mode3**

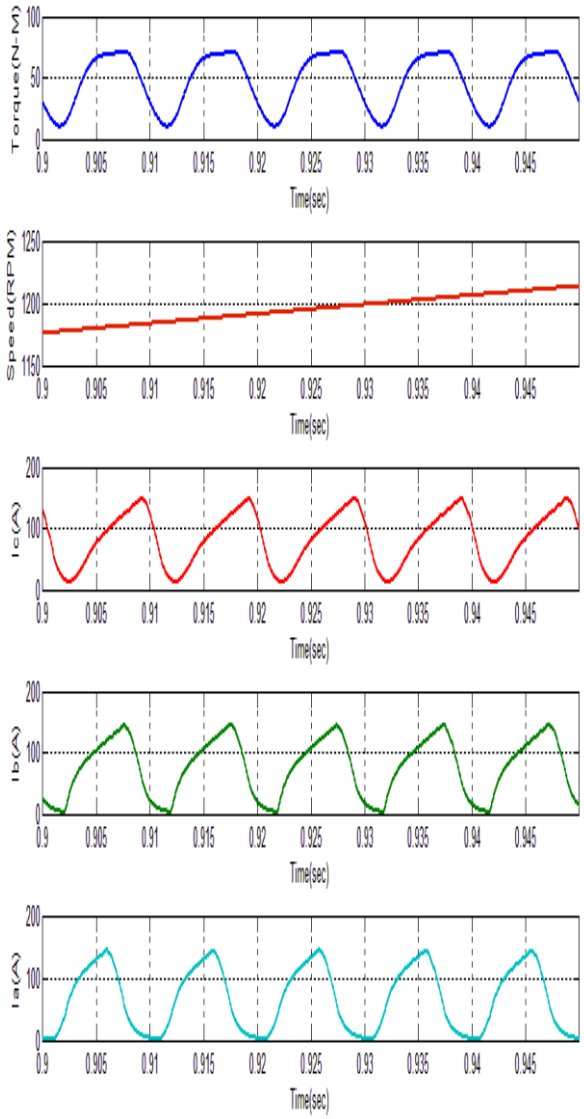


**(b) Simulation results of single source driving mode (modes 3)**

**Fig. 15 Simulation results for driving conditions at modes 1, 3 and 4.**

**Mode 5**

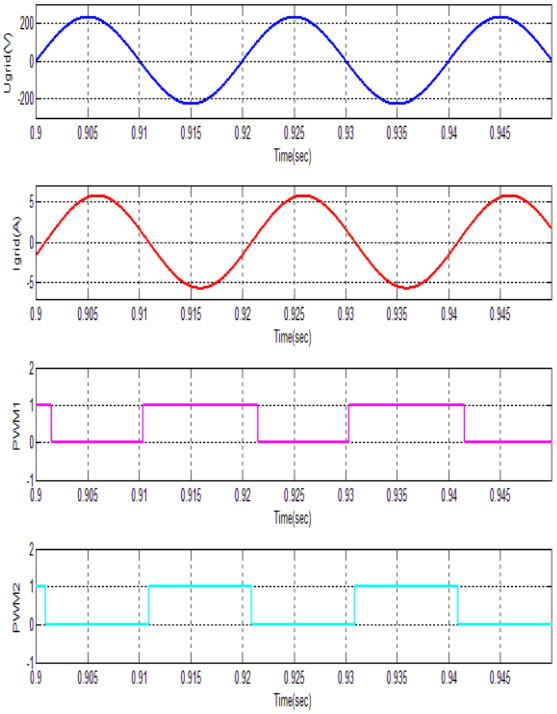


**Mode6_Stage1**

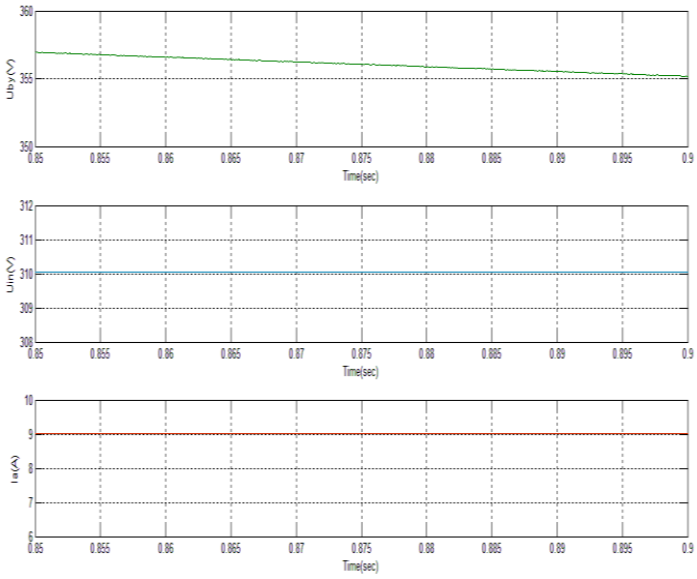


**(b) PV charging mode 6 (stage 1)**

**Mode6_Stage2**

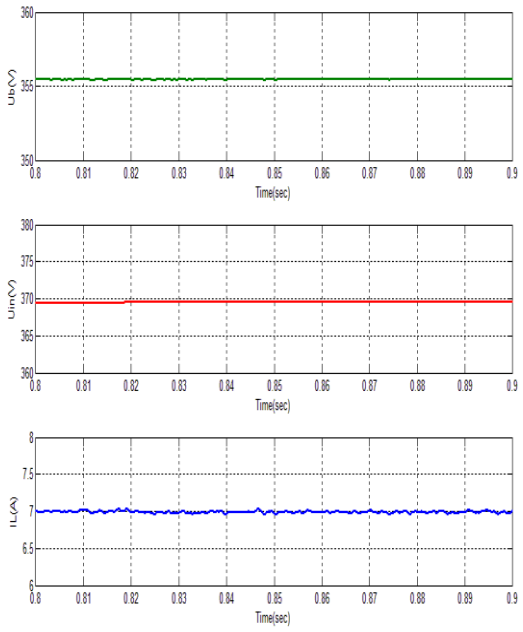


**(c) PV charging mode 6 (stage 2)**

**Mode6_Stage3**

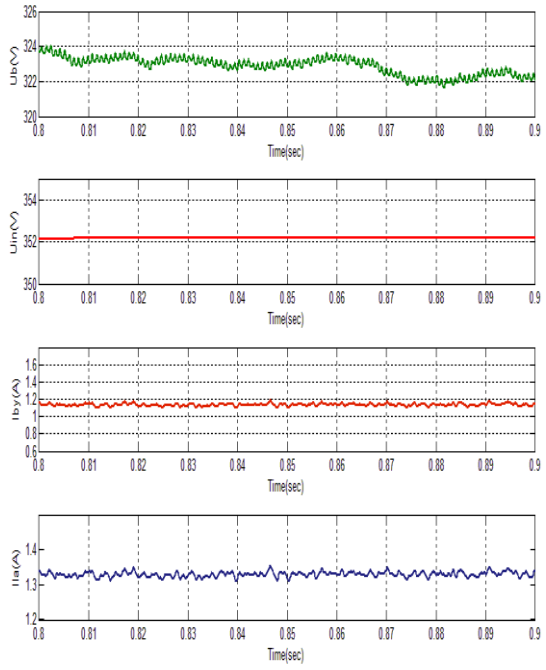


**(d)PV charging mode 6 (stage 3)**

**Fig. 16 simulation results for charging modes.**

**Table III: THD values for Proposed and Extension methods.**

| THD in % Existing Method | THD in % Extension Method |
|---|---|
| **Mode 1:** $I_a$= 41.43, $I_b$ =38.12, $I_c$=64.58 | **Mode 1:** $I_a$= 25.72, $I_b$ =19.82, $I_c$=27.12 |
| **Mode 2:** $I_a$= 43, $I_b$ =31.01, $I_c$=71.52 | **Mode 2:** $I_a$= 26.66 , $I_b$ =17.68 , $I_c$=30.04 |
| **Mode 3:** $I_{La}$= 82.66, $I_{Lb}$ =33.68, $I_{Lc}$=43.47 | **Mode 3:** $I_{La}$= 51.25, $I_{Lb}$ =17.51, $I_{Lc}$=18.26 |
| **Mode 4:** $I_{La}$= 64.68, $I_{Lb}$ =34.25, $I_{Lc}$=41.87 | Mode 4: $I_{La}$= 40.1, $I_{Lb}$ =17.81, $I_{Lc}$=17.58 |
| **Mode 5:** $U_{grid}$ = 0.004535,$I_{grid}$ =0.004864 | **Mode 5:** $U_{grid}$ = 0.004535,$I_{grid}$ =0.004864 |
| **Mode 6:stage 1** $I_a$= 11.5 | **Mode 6:stage 1** $I_a$= 4.091 |
| **Mode 6:stage 2** $I_{La}$= 2.377 | **Mode 6:stage 2** $I_{La}$= 0.9985 |
| **Mode 6:stage 1** $I_a$= 2.429,$I_b$=2.632 | **Mode 6:stage 3** $I_a$= 2.546,$I_b$=1.608 |

## VI. CONCLUSION

In order to handle the range anxiety of utilizing EVs and decrease the system cost, a mix of the PV panel and SRM is proposed as the EV driving system.

The main contributions of this paper are:

(i) A Tri-port converter is utilized to associate the PV panel, battery and SRM.

(ii) Six working modes are produced to accompli sh adaptable energy stream for controlling the driving, charging and hybrid (i.e., mix of both driving and charging) modes.

(iii) An exceptional charging topology is proposed such that the vehicle can be charged from the grid with no outside power electronic gadgets

(iv) Photo Voltaic encouraged battery charging control game plan is created alongside irritate and watch MPPT to propel the usage of sunlight based energy.

(v) ANFIS controller is fused to control the general operations and to lessen the aggregate consonant mutilations.

Since PV-fed EVs are a greener and more economical innovation than conventional ICE vehicles, this work will give feasible solution to reducing the total costs and CO2emissions of electrified vehicles. Moreover, the proposed innovation may likewise be connected to comparable applications, such asfuel cell powered EVs. Fuel cells have a considerably higher power density and are hence more qualified for EV applications.

**REFERENCES**

[1] A. Emadi, L. Young-Joo, K. Rajashekara, "Power electronics and motor drives in electric, hybrid electric, and plug-in hybrid electric vehicles," IEEE Trans. Ind. Electron., vol. 55, no. 6, pp. 2237-2245, Jun. 2008.
[2] B. l. K. Bose, "Global energy scenario and impact of power electronics in 21st century," IEEE Trans. Ind. Electron., vol. 60, no. 7, pp. 2638-2651, Jul. 2013.
[3] J. de Santiago, H. Bernhoff, B. Ekergård, S. Eriksson, S. Ferhatovic, R. Waters, and M. Leijon,"Electrical motor drivelines in commercial all-electric vehicles: a review," IEEE Trans. Veh. Technol., vol. 61, no. 2, pp. 475-484, Feb. 2012.
[4] Z. Amjadi, S. S. Williamson, "Power-electronics-based solutions for plug-in hybrid electric vehicle energy storage and management systems," IEEE Trans. Ind. Electron., vol. 57, no. 2, pp. 608-616, Feb. 2010.
[5] A. Kuperman, U. Levy, J. Goren, A. Zafransky, and A. Savernin, "Battery charger for electric vehicle traction battery switch station," IEEE Trans. Ind. Electron., vol. 60, no. 12, pp. 5391-5399, Dec. 2013.

**Authors Biography:**

**Mr.G.Varshith** from Tirupathi, Andhra Pradesh who has a zeal in research participated in various activites since childhood. He is a Graduate in the Stream of Electrical & Electronics Engineering from Sree Vidyanikethan Engineering College – An Autonomous Institute affiliated to JNTU Ananthapur.

**Mr. B.Pavan Kumar Reddy** from Tirupathi, Andhra Pradesh completed his Graduation in the stream of Electrical and Electronics Engineering (EEE) from Sree Vidyanikethan Engineering College in 2014. He gained Practical knowledge by working as Maintenance Engineer at Amara Raja Batteries Limited for a 15 Months and recently completed his masters in Power Electronics and Electrical Drives specialization from VEMU Institute of Technology – An ISO 2015:9001 certified institute affiliated to JNTU Ananthapur.

**Miss B.Kavya Sree Reddy** from Tirupathi, Andhra Pradesh had shown her merit in many exams conducted by various institutes & stood top in them. Presently pursuing her graduation in the stream of Electrical & Electronics Engineering from National Institute of Technology, Puducherr y**(NITPY).**